Inorganic Chemistry
Article

Inorg. Chem. **2009,** *48,* 4729–4736 **4729**
DOI:10.1021/ic802319c

Ligand-Driven Light-Induced Spin Change Activity and Bidirectional Photomagnetism of Styrylpyridine Iron(II) Complexes in Polymeric Media

M.-L. Boillot,*,† S. Pillet,‡ A. Tissot,† E. Rivière,† N. Claiser,‡ and C. Lecomte‡

†*ICMMO, ECI, UMR CNRS 8182, Université Paris-Sud 11, 91 405 Orsay, France and* ‡*CRM2, Nancy-Université, CNRS, Boulevard des Aiguillettes, B.P. 239, 54506 Nancy, France*

Received December 3, 2008

Two pseudo-octahedral iron(II) complexes, $Fe(stpy)_4(NCSe)_2$, containing photoresponsive ligands (cis ↔ trans isomerization of −CH═CH−) were prepared with *trans*- or *cis*-styrylpyridine (stpy) isomers. The magnetic behavior of the polycrystalline solids was previously shown to depend on the configuration of the stpy ligand. The crystal X-ray structures were determined at 293 and 104 K for both isomers. The all-trans and all-cis compounds crystallize in the orthorhombic ($Pna2_1$) and the monoclinic space groups ($C2/c$), respectively. No symmetry change occurs upon cooling to 104 K. The Fe(II) centers lie in axially compressed octahedra with NCSe anions in the apical position and the four pyridinic nitrogens in the meridional plane. The variation of metal−ligand bond lengths as a function of temperature reflects the thermal $S = 0 \leftrightarrow S = 2$ crossover of all-trans complexes and the $S = 2$ ground state of all-cis complexes. The unit-cell volumes per metal ion also change accordingly, and the relative variation due to the spin-crossover compares those associated with the formal change of configuration of the four stpy isomers. The photomagnetic responses were investigated at 130 K with doped polymer thin films containing all-cis (high-spin) or all-trans species (partly low-spin). The 130 K illumination of these doped poly(methyl methacrylate) (PMMA) films leads to the UV−vis absorption features typical for the cis ↔ trans photoisomerization of the stilbenoid moiety. The direct magnetic measurements have unambiguously established the photomagnetic effect named ligand-driven light-induced spin change (LD-LISC). The 355 nm excitation of doped thin films produces very long lifetime states that are manifested by high-spin to low-spin (all-cis complex) and low-spin to high-spin (all-trans complex) changes of the Fe(II) magnetic behavior; the process is bidirectional. A structural analysis based on the single-crystal X-ray diffraction data has been proposed to rationalize the LD-LISC activity detected here for doped PMMA thin films.

Introduction

There is currently active interest in the development of inorganic systems based on the interaction between transition metal ions and photoresponsive ligands.[1−5] The possibility to tune the organic photoactivity by metal coordination has been explored in inorganic photochemistry for producing original pathways for photoexcitation and relaxation as well as dynamics.[2] Combinations of photochromism and some transition metal complexes' functionalities have been selected for elaborating multimode photofunctional molecules.[3−5] Various photochemical processes (for example, isomerization, cyclization, proton transfer, etc.) with thermally reversible or irreversible characteristics have been applied to modulate the organic part's properties. Transition metal ions of the second and third series have been frequently preferred, undoubtedly because of their specific redox and photophysical characteristics.

Some years ago, we described how a high-spin (HS) ↔ low-spin (LS) conversion of an Fe^{II} ion could be controlled through the trans−cis photoisomerization of the styrylpyridine ligand. For this photomagnetic effect, named ligand-driven light-induced spin change (LD-LISC),[6] light irradiation switches the stilbenoid configuration, and the subsequent modulation of the Fe^{II} electronic environment may be strong enough to change the spin state of the spin-crossover metal ion. These latter molecular materials are nice prototypes of bistable systems whose LS ↔ HS state conversion of

*To whom correspondence should be addressed. E-mail: mboillot@icmo.u-psud.fr.

(1) (a) Zarnegar, P. P.; Bock, C. R.; Whitten, D. G. *J. Am. Chem. Soc.* **1973**, *95*, 4367. (b) Wrighton, M. S.; Morse, D. L.; Pdungsap, L. *J. Am. Chem. Soc.* **1975**, *97*, 2073.
(2) (a) Vlcek, A.; Busby, M., Jr. *Coord. Chem. Rev.* **2006**, *250*, 1755. (b) Bossert, J.; Daniel, C. *Chem. Eur. J.* **2006**, *12*, 4835. (c) Polo, A. S.; Itokazu, M. K.; Frin, K. M.; Patrocínio, A. O. D.; Iha, N. Y. M. *Coord. Chem. Rev.* **2006**, *250*, 1669.
(3) Matsuda, K.; Irie, M. *J. Photochem. Photobiol. C* **2004**, *5*, 169.
(4) (a) Kume, S.; Nishihara, H. *Struct. Bonding*; Springer: New York, **2007**; Vol. *123*, pp 79−112. (b) Kume, S.; Nishihara, H. *Dalton Trans.* **2008**, *25*, 3260.
(5) Fraysse, S.; Coudret, C.; Launay, J.-P. *Eur. J. Inorg. Chem.* **2000**, 1581.
(6) (a) Roux, C.; Zarembowitch, J.; Gallois, B.; Granier, T.; Claude, R. *Inorg. Chem.* **1994**, *33*, 2273. (b) Boillot, M.-L.; Roux, C.; Audière, J.-P.; Dausse, A.; Zarembowitch, J. *Inorg. Chem.* **1996**, *35*, 3975.

Published on Web 4/17/2009

the metal center is triggered by physical (T, P, H, and hν) or chemical stimuli (solvent, gaz, etc).[7] The photoswitching of spin-crossover materials may be observed by the direct excitation of the metal ion (dd or MLCT excitation) according to the light-induced excited spin state trapping (LIESST).[8] For LIESST materials (mainly Fe^{II} compounds), the electronic relaxation following the LS photoexcitation takes place through the structural rearrangement of the metal ion environment. This favors a quantitative trapping of the metastable HS state at sufficiently low temperatures. For LD-LISC materials, the thermal energy barrier between the two ligand isomers is chosen to be large enough to ensure a very long lifetime of the metal ion's spin states, a priori at room temperature. Therefore, various characteristics related to the metal center (for example, optical, dielectric, magnetic, or vibrational) can be used for a nondestructive readout of the spin state bistability. The photomagnetic effect was reported first for Fe(II) and Fe(III) complexes bearing a −CH=CH− pyridine group; different characteristics, such as the working temperature, were shown to be tuned by appropriate molecular components.[9] These findings have established that the LD-LISC approach provides a rational method for the design and elaboration of ultra-high-density molecular memories or optical devices.

Furthermore, different questions about the LD-LISC mechanism, the dynamic properties, and the effect of a confined environment on the underlying processes can be raised. It has been anticipated that ultrafast time-resolved techniques coupled to magneto-optical measurements might be very efficient tools for detecting and analyzing the LD-LISC process in highly diluted and transparent polymeric thin films. The optical magnetic circular dichroism (MCD) investigation of a new set of compounds, $Fe(stpy)_4(NCSe)_2$ (stpy = *cis*- and *trans*-styrylpyridine isomers), was recently reported.[10] Finally, ab initio and molecular dynamic methods were used for an in-depth description of the more simple LD-LISC ligand−4-styrylpyridine−in its ground state.[11]

We focus here on the switching (optical and magnetic) and structural properties of $Fe(stpy)_4(NCSe)_2$ (called all-trans or all-cis compounds according to the ligands' configurations), the studied samples being either the crystalline molecular solids or the poly(methyl methacrylate) (PMMA) polymeric films doped with the coordination compounds.

Experimental Section

Orange−red single crystals were isolated by slow evaporation of a $MeOH/H_2O$ solution of all-trans and all-cis complexes.

The doped-polymer thin film samples consisted of PMMA containing x% of the all-cis or all-trans complex (x = 2−20 wt %). In a typical procedure, 40 mg of PMMA and 2 mg of the Fe(II) complex were dissolved in 0.5 mL of chloroform and spin-coated onto fused silica substrates.

X-Ray Diffraction Measurements and Structure Determination. In order to correlate the differences in magnetic behavior to the structural characteristics of the two isomers, their crystal structures were determined at two temperatures, namely, 293 and 104 K, well above and below the thermal spin transition of the all-trans solid, respectively. Single-crystal X-ray diffraction measurements were performed using an Oxford Diffraction Xcalibur diffractometer with Mo(Kα) radiation, equipped with a Sapphire-2 CCD detector and a N_2 open flow cryostream for low-temperature measurements. It was previously reported that the thiocyanate parent derivatives exhibit significant crystal damage upon daylight exposure.[6] Special care was thus attached to crystal selection and mounting under the microscope with reduced light; all diffraction measurements have been carried out in complete darkness. The diffraction peaks were integrated using the CRYSALIS software.[12] Cell parameters were derived using a least-squares refinement on all measured reflections. The crystal faces were indexed to perform analytical absorption corrections. All structures were solved by direct methods and refined on F^2 using a similar strategy (SHELXL97).[13] Non-hydrogen atoms were refined anisotropically; hydrogen atoms were generated at their ideal positions. For $Fe(trans\text{-}stpy)_4(NCSe)_2$ at room temperature, the structure refinement clearly indicated a disorder on one of the selenium atoms. This disorder has been described using a split atomic position and constraining the anisotropic displacement parameters of the major and minor Se positions to be identical. Similarly, a disorder on the central ethylenic function of two of the styrylpyridine ligands has been identified and described in the refinement. Structure solution and refinement in monoclinic subgroups have been attempted to solve the disorder; this strategy did not lead to any significant improvement in the quality of the structural model. Such a disorder is not uncommon and does not alter nor influence the conclusions drawn hereafter.

Photocrystallographic measurements have been attempted on single crystals using 330−360 nm excitation from an Ar−Kr gas laser ($P \sim 20$ mW) at both 293 and 104 K. The samples were continuously rotated to ensure a homogeneous excitation. However, the crystal structures after excitation did not reveal any significant structural modification. The high extinction coefficients of the $\pi-\pi^*$ transitions of the stpy ligand result in penetration depths which are far too small to allow an efficient bulk excitation of the samples; only the surface of the crystals was most probably excited during these experiments.

Alternatively, X-ray diffraction experiments have been conducted on powder samples using synchrotron radiation. On the basis of the UV−vis absorption spectra of the cis and trans forms, the samples were excited at 254 and 365 nm, respectively, using a filtered Hg lamp at room temperature. Despite very long irradiation times and different crushing intensities, the recorded powder spectra did not show any measurable modification, indicating the absence of significant trans → cis or cis → trans photoisomerization. A similar experiment was carried out on the base-free ligand (365 nm) without measurable effects.

UV−Vis Measurements. The low-temperature absorption measurements of the doped-polymer thin film were performed using a Varian Cary 5E double-beam spectrophotometer equipped with an APD Cryogenics closed-cycle helium cryogenic system including a DMX-1E cryostat and a DE-202 expander. Ex situ UV−vis irradiation was carried out with a 200 W Oriel arc lamp (Xe/HgXe) and filters (340FS25−25, 313FS10−50, 254FS10−50).

(7) Gütlich, P.; Goodwin, H. A. *Topics in Current Chemistry*; Springer : Berlin, 2004; Vols. 233−235.
(8) Hauser, A. *Topics in Current Chemistry*; Gütlich, P., Goodwin, H. A., Eds.; Springer: Berlin, 2004; Vol. 234, pp 155−198.
(9) (a) Boillot, M.-L.; Zarembowitch, J.; Sour, A. *Topics in Current Chemistry*; Gütlich, P., Goodwin, H. A., Eds.; Springer: Berlin, 2004; Vol. 234, pp 261−276. (b) Boillot, M.-L.; Chantraine, S.; Zarembowitch, J.; Lallemand, J.-Y.; Prunet, J. *New J. Chem.* **1999**, *23*, 179. (c) Sour, A.; Boillot, M.-L.; Rivière, E.; Lesot, P. *Eur. J. Inorg. Chem.* **1999**, 2117.
(10) Kolb, J. S.; Thomson, M. D.; Novosel, M.; Sénéchal-David, K.; Rivière, E.; Boillot, M.-L.; Roskos, H. G. *C.R. Chim.* **2007**, *10*, 125.
(11) Lawson Daku, L. M.; Linarès, J.; Boillot, M.-L. *ChemPhysChem.* **2007**, *8*, 1402.
(12) *CrysAlis CCD*; *CrysAlis RED*, versions 1.171; Oxford Diffraction: Wroclaw, Poland, 2004.
(13) Sheldrick G. M. *SHELX97*; University of Gottingen: Germany, 1997.

Magnetization Measurements. Magnetization measurements were carried out on microcrystals using a Quantum Design SQUID magnetometer (MPMS5S model) calibrated against a standard palladium sample. The magnetization versus the magnetic field data were collected in the 2−300 K temperature range within a 0−5 T magnetic field. For photoexcitation of the solids, the magnetometer was equipped with an optical fiber (UV grade fused silica) connected to a Surelite-Continuum Performance Nd:YAG pulsed laser (ranging from 450 to 800 mJ at 1064 nm and harmonic options for 532 and 355 nm outputs). In situ excitations were performed with λ = 355 nm (~5 mW/cm^2). Negative values of magnetization are observed as a consequence of prevailing contributions of substrate and PMMA polymer.

Results and Discussion

1. Magnetic Behavior of Polycrystalline Samples. Figure 1 shows the temperature dependence of $\chi_M T$ (χ_M, molar magnetic susceptibility; T, temperature) of microcrystalline samples of all-trans and all-cis complexes.[10] The all-trans complex exhibits a rather gradual and complete low-spin (S = 0) ↔ high-spin (S = 2) spin-crossover process centered at $T_{1/2}$ = 163 K. The all-cis complex retains the S = 2 ground state at any temperature. The corresponding $\chi_M T$ versus T curve is typical for hexacoordinated iron(II) ions whose orbital degeneracy of the $^5T_{2g}$ term is partly removed under the effect of the low-symmetry component of the ligand field. The zero-field splitting parameters were obtained by fitting the magnetization versus field curves (see Figure S1, Supporting Information). The best-fitted values (D = 5.3 cm^{-1}, E/D = 0.18 and g = 2.03) are in satisfying agreement with the data extracted from MCD for this polymer thin film.[10]

These magnetic behaviors compare to those previously reported for several analogs Fe(stpy)$_4$(X)$_2$ (X$^-$ = NCS, NCBPh$_3$, NCBH$_3$).[6] Within this series, the metal ion's electronic environment is mainly determined by the styrylpyridine isomer. The larger ligand field strength observed with *trans*-stpy is accounted for by its almost planar structure, which favors an efficient electronic delocalization and a significant stabilization of its π and π^* orbitals. Additional modulations due to the axially linked anions are observed in the spin-crossover characteristics of all-trans compounds.

The actual stilbenoid configuration dependence follows the criteria for LD-LISC, and as such, we can investigate how the photoswitching of coordinated stpy occurs in convenient media and probe the LD-LISC activity of these Fe(II) complexes.

2. X-Ray Crystal Structures. The all-cis and all-trans compounds crystallize in the monoclinic $C2/c$ and orthorhombic $Pna2_1$ space groups, respectively. In both cases, no symmetry change occurs upon cooling to 104 K. For the all-trans compound, the asymmetric unit comprises one crystallographically independent molecule, Fe(stpy)$_4$(NCSe)$_2$, while for the all-cis, the molecule is sitting on a 2-fold axis. The asymmetric unit thus consists of half a molecule. The molecular structures at 293 K are shown in Figure 2; relevant crystallographic data are collected in Tables 1 and 2.

Let us first discuss the structures at 293 K, at which the two isomers are in the HS state. In both cases, the iron(II) ion lies in an axially compressed octahedron with two

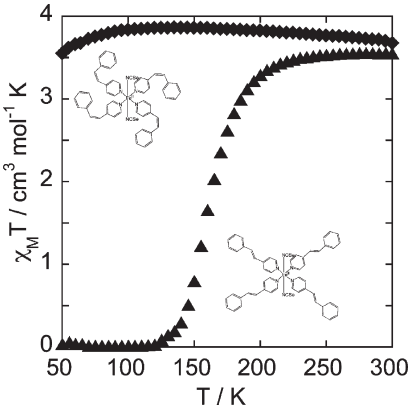

Figure 1. Temperature dependence of $\chi_M T$ for polycrystalline samples of Fe(*trans*-stpy)$_4$(NCSe)$_2$ and Fe(*cis*-stpy)$_4$(NCSe)$_2$.

selenocyanato groups in the apical position and four nitrogen atoms of pyridinic rings in the basal plane. The distortions of the [FeN$_6$] coordination core are reflected in the bond lengths and bond angles (Table 2), with the Fe−N(CSe) bonds being 0.08−0.14 Å shorter than the corresponding Fe−N(stpy) ones. A similar situation was also evidenced for the parent materials Fe(stpy)$_4$(NCS)$_2$.[6] Both sets of parameters, in the all-cis and all-trans forms, are usual for iron ions in the high-spin electronic configuration.[14] It is noteworthy that the angular distortion of the [FeN$_6$] octahedron, characterized by the Σ parameter, is higher than typically characterized for FeL$_4$(NCS)$_2$ spin-crossover materials;[14] this distortion is even higher for the all-cis form (Σ_{cis} = 36.2°, Σ_{trans} = 22.0°), which correlates with the higher average Fe−N bond length ($<$Fe−N$>_{cis}$ = 2.201 Å, $<$Fe−N$>_{trans}$ = 2.187 Å).

The NCSe anions are coordinated to the iron ion in a bent fashion (160.2(2)−175.9(2)°). Consistently, the N−C bond lengths at 1.125(5)−1.157(4) Å indicate the sp^2 hybridization of nitrogen atoms, while the C−Se bond lengths (1.785(4)−1.792(5) Å) are between the values expected for single and double bonds. The NCSe ligands are almost linear (171−179°), with the apparent exception of N1−C1−Se$_i$ (i = 1 or 3) in the all-trans molecule at 293 K, which is nevertheless meaningless, owing to the statistical position disorder of the terminal Se atom.

a. Configuration Analysis. For both isomers, different geometries are adopted by the pyridyl moieties, especially a tilt with regard to the meridional average plane [FeN$_4$] (Table S1, Supporting Information) minimizing interring sterical hindrance, and accordingly very low symmetries are observed in the coordination cores. This arrangement around the metal ion restricts the π-stacking of *trans*-stpy ligands and leads to four distinct trans (and two distinct cis) configurations of the stpy isomers. The arrangement is almost symmetric for the trans form (pseudopropeller), while the cis compound adopts a highly asymmetric configuration. The dihedral angles C(Ph)−CH=CH−C(py) of the ethylenic fragment (Table S1, Supporting Information) vary in the ranges 171.2−178.5° and 8.1−9.5° for the trans and cis isomers, respectively (for consistency, the C$_{Ph}$−C1−C2−C$_{py}$ notation

(14) Guionneau, P.; Marchivie, M.; Bravic, G.; Létard, J.-F.; Chasseau, D. *Topics in Current Chemistry*; Gütlich, P., Goodwin, H. A., Eds.; Springer: Berlin, 2004; Vol. 234, p 97−128.

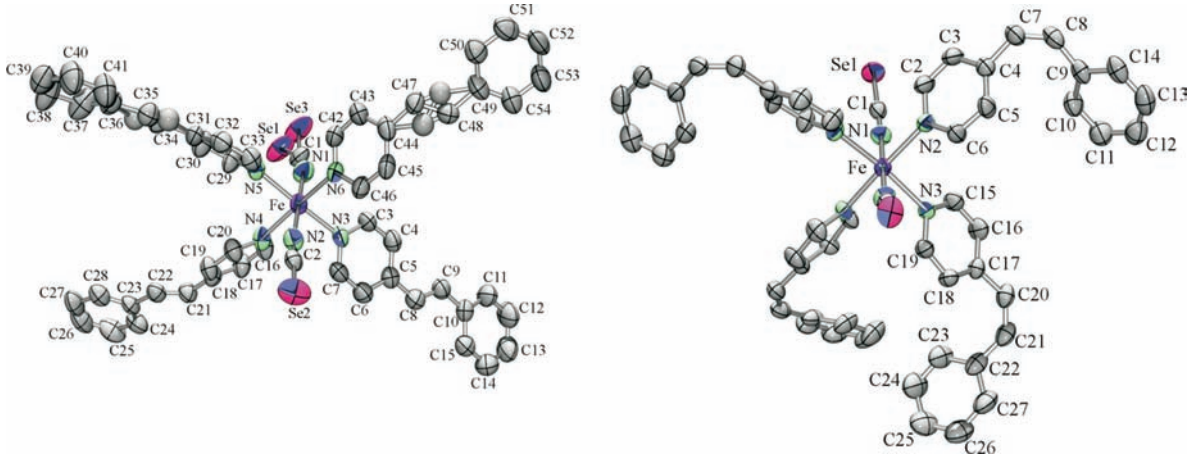

Figure 2. Molecular structures of all-trans (left) and all-cis (right) complexes of $Fe(stpy)_4(NCSe)_2$ at 293 K (ORTEP plot with 50% probability ellipsoids).

Table 1. Crystal Data and Structure Refinement Details for $Fe(stpy)_4(NCSe)_2$

	all-cis		all-trans	
empirical formula	$C_{54}H_{44}N_6Se_2Fe$		$C_{54}H_{44}N_6Se_2Fe$	
fw/g mol^{-1}	990.72		990.72	
T/K	104(2)	293(2)	104(2)	293(2)
cryst syst	monoclinic	monoclinic	orthorhombic	orthorhombic
space group	$C2/c$	$C2/c$	$Pna2_1$	$Pna2_1$
a/Å	19.593(1)	19.748(1)	31.865(2)	32.326(2)
b/Å	13.217(1)	13.253(1)	15.195(1)	15.382(1)
c/Å	18.058(1)	18.335(1)	9.7180(6)	9.9414(6)
β/deg	94.650(4)	95.081(5)	90	90
V/Å^3	4660.9	4779.8	4705.2	4943.3
Z	4	4	4	4
ρ_{calc}/g cm^{-3}	1.41	1.38	1.40	1.33
μ/mm^{-1}	1.93	1.88	1.91	1.82
measured data	28050	16502	60206	28820
$(\sin\theta/\lambda)_{max}$	0.71	0.60	0.71	0.60
R_{int}[a]	0.055	0.047	0.035	0.040
independent data	7008	4380	13809 [d]	8999 [d]
wR2 [$F^2 > 2\sigma(F^2)$][b]	0.104	0.109	0.082	0.091
R1 [$F^2 > 2\sigma(F^2)$][c]	0.048	0.047	0.035	0.038

[a] $R_{int} = \sum(N/N-1)\sum_i|I_i - <I>|/\sum\sum_i I_i$. [b] wR2 = $(\sum[w(F_o^2 - F_c^2)^2]/\sum[w(F_o^2)^2])^{1/2}$. [c] R1 = $\sum||F_o| - |F_c||/\sum|F_o|$. [d] For the all-trans compound, Friedel pairs were not merged, owing to the significant anomalous dispersion effect from Se and Fe in the noncentrosymmetric $Pna2_1$ space group.

Table 2. Structural Parameters of the [Fe−N_6] Octahedron for the all-cis and all-trans Forms at 293 and 104 K

	all-cis		all-trans	
	104 K	293 K	104 K	293 K
Fe−N1 (Å)	2.148(2)	2.143(3)	1.938(2)	2.093(4)
Fe−N2 (Å)	2.217(2)	2.226(3)	1.944(2)	2.138(4)
Fe−N3 (Å)	2.221(2)	2.234(3)	1.999(2)	2.225(3)
Fe−N4 (Å)			2.009(2)	2.237(4)
Fe−N5 (Å)			2.006(2)	2.220(3)
Fe−N6 (Å)			2.003(2)	2.212(4)
<Fe−N>	2.195	2.201	1.983	2.187
Σ (deg)[a]	35.1	36.2	14.3	22.0

[a] Σ is defined as the sum of the absolute values of the deviation from 90° of the 12 cis angles in the coordination sphere.

will be used hereafter, as in ref 11). These values deviate from those reported[15] or calculated[11] for the base-free ligands (179.1 or 180° for *trans*-stpy and 6.6° for *cis*-stpy), owing to complexation effects with the central Fe(II) ion and most likely to the influence of the crystal packing, the calculations being performed on isolated molecules in the gas phase. Especially, the trans isomer deviates by as much as 10° from the ideal planar geometry, this latter being attributed to an efficient delocalization of the π system over the whole ligand (aromatic rings connected by the ethylenic central function), as revealed in the DFT calculations. Although $Fe(trans\text{-}stpy)_4(NCSe)_2$ is isostructural with its parent sulfur derivative $Fe(trans\text{-}stpy)_4(NCS)_2$, the configuration of the four stpy ligands differs. In the present case, two of the four ligands exhibit negative and close to 180° $C_{Ph}-C1-C2-C_{py}$ dihedral angles (178.5(5)° and 175.3(5)°), while for the remaining two ligands, the dihedral angle is positive (171.9(4)° and 171.2(4)°) and deviates much from 180°. The angle between the least-squares planes of the pyridine and phenyl rings corresponds to mean values of 13.5 and 41.5°, respectively, for each situation, obviously in departure from the null value for a planar geometry, as evidenced in the DFT calculations for the base-free ligand. Interestingly, the two most planar stpy ligands are arranged apart from the central Fe(II) ion in the coordination sphere. As

(15) Cariati, E.; Roberto, D.; Ugo, R.; Srdanov, V. I.; Galli, S.; Macchi, P.; Sironi, A. *New J. Chem.* **2002**, *26*, 13.

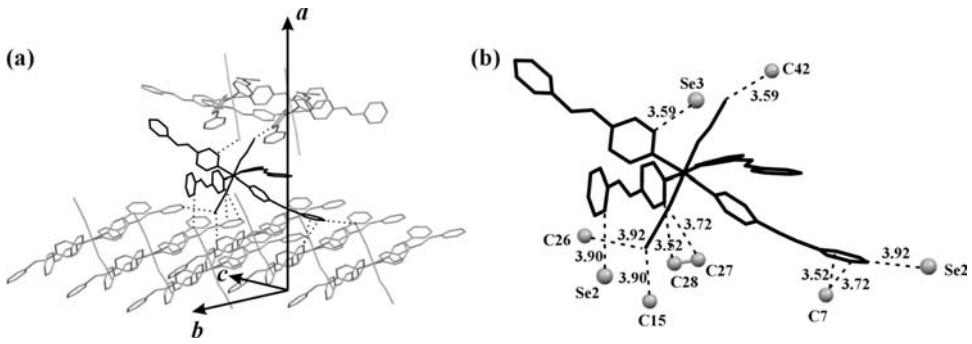

Figure 3. Crystal packing and intermolecular contacts between a central molecule (in black) and the closest neighbors (in gray) for Fe(*trans*-stpy)$_4$(NCSe)$_2$ (T = 293 K). The numbers indicate intermolecular distances in ångstroms.

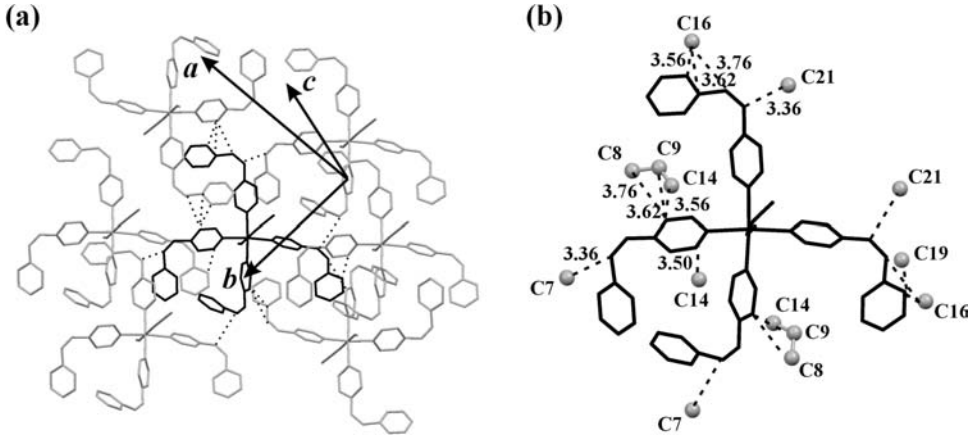

Figure 4. Crystal packing and intermolecular contacts between a central molecule (in black) and the closest neighbors (in gray) for Fe(*cis*-stpy)$_4$(NCSe)$_2$ (T = 293 K). The numbers indicate intermolecular distances in ångstroms.

a whole, it is thus observed that *trans*-stpy exhibits a certain torsion disparity around the central C=C ethylenic bond in the crystalline phase. In the case of the cis isomer, both stpy ligands exhibit similar structural geometries, with a positive $C_{Ph}-C1-C2-C_{py}$ dihedral angle and a quite large angle between the least-squares planes of the pyridine and phenyl rings which amounts to 50.5° on average. This distortion originates from steric hindrance effects between the neighboring ortho H substituents of the two rings and barely results from packing effects. It has been suggested from the DFT calculations that the trans → cis isomerization gives rise to systematic structural differences, such as a 4° increase in the $C_{Ph}-C1-C2$ and $C1-C2-C_{py}$ angles together with a 0.01 Å lengthening of the $C_{Ph}-C1$ and $C2-C_{py}$ bonds, while the central C1−C2 should not be affected. The corresponding trans → cis differences we derive here indicate indeed an increase in the $C_{Ph}-C1-C2$ and $C1-C2-C_{py}$ angles (from 125.7° to 132.6° in average), accompanied by a slight increase in the C1−C2 bond length (from 1.294 to 1.327 Å on average), while the $C_{Ph}-C1$ and $C2-C_{py}$ bonds do not show any systematic trend. Although the calculations have been performed on base free ligands as opposed to a crystalline and coordinated situation in the Fe(stpy)$_4$(NCSe)$_2$ complexes, the main structural features are indeed observed experimentally.

b. Intermolecular Interactions and Crystal Packing. The crystal packing of the trans isomer is identical to that reported for the sulfur derivative, while the packing of the cis form is clearly different. As shown in Figures 3 and 4, the cohesion of both solid structures is achieved by numerous, although rather weak, contacts between neighboring molecules involving the NCSe groups and the aromatic rings of stpy, such as Se···H−C hydrogen bonds, π-stacking in a T-shaped arrangement, or close C···C interactions. It does not involve any significant intermolecular π-stacking with a parallel configuration. The shortest intermolecular contacts are collected in Tables 3 and 4. For the trans form, three of the four stpy ligands and the two NCSe groups are involved in distinct intermolecular contacts, which are less numerous than in the parent Fe(*trans*-stpy)$_4$(NCS)$_2$ material. This can be well understood since the unit cell volume is almost 100 Å^3 smaller for this latter one, and thus molecules are more densely packed.

Shorter C···C distances are observed between the stpy ligands of the cis form. As evidenced in the packing diagram (Figure 4), the orientation of the cis ligands seems quite fixed in the solid state, since both aromatic rings are involved in intermolecular close contacts. Contrary to the trans materials, the sulfur and selenium derivatives of the cis form exhibit very similar unit cell volumes (taking into account the different space groups) and therefore intermolecular contacts within the same range of distances.

c. Low-Temperature Structures. Upon cooling to 104 K, the cis isomer retains its high-spin state. Accordingly, for this isomer, the structural modifications characterize only thermal contraction effects: a slight shortening of the coordination Fe−N distances (from 2.201 to 2.195 Å for

Table 3. Intermolecular Distances Shorter than the Sum of the van der Waals Radii for Fe(*trans*-stpy)$_4$(NCSe)$_2$ at 293 and 104 K

	all-trans 104 K	all-trans 293 K
Se3···C42	3.544(2)	3.593(5)
Se2···C15	3.829(3)	3.907(5)
Se2···C26	3.845(3)	3.925(8)
C7···C27	3.614(3)	3.719(7)
C7···C28	3.419(3)	3.517(6)

Table 4. Intermolecular Distances Shorter than the Sum of the van der Waals Radii for Fe(*cis*-stpy)$_4$(NCSe)$_2$ at 293 and 104 K

	all-cis 104 K	all-cis 293 K
C19···C14	3.387(3)	3.501(5)
C21···C7	3.298(3)	3.365(5)
C16···C8	3.681(3)	3.757(5)
C16···C9	3.578(3)	3.622(5)
C16···C14	3.518(4)	3.560(5)

$<$Fe$-$N$>$), while the bond distances and angles within the NCSe and stpy ligands are only marginally affected. The conformation of the stpy ligands remains unaffected; the $C_{Ph}-C1-C2-C_{py}$ torsion angles only slightly increase. The most significant reorganization concerns the larger tilt of the pyridyl moieties with regard to the meridional average plane [FeN_4] (from 34.1° to 38.0° on average). Contrary to the cis form, the trans isomer undergoes a high-spin to low-spin transition centered at $T_{1/2}$ = 163 K. The related structural reorganization can be pictured as a global contraction of all of the Fe$-$N bonds by 0.204 Å, which is a typical value for $FeL_4(NCS)_2$ spin-crossover materials.[6] In parallel, the [FeN_6] octahedron becomes more regular in the low-spin state, as revealed by the decrease in the angular distortion parameter Σ from 22 to 14°. The conformation of the *trans*-stpy ligands is only marginally affected by the spin transition; in particular, the sign of the $C_{Ph}-C1-C2-C_{py}$ torsion angles is retained.

d. Free Cavity Space and Possibility for Solid-State Isomerization. There are now many examples which demonstrate that organized and constraining media, such as a crystalline phase, influence the ability of a guest molecule to undergo a photochemical reaction and may even control the reaction rate.[16] Specific concepts of a reaction cavity and free volume have been defined;[16] these are often used to rationalize the occurrence or absence of a solid-state reaction. As the reaction proceeds, the reaction cavity must be able to accommodate the reactant-to-product structural reorganization, and as such, excess free volume is obviously required around the reaction site in the crystal packing. Cis$-$trans photoisomerization is a representative example of such a high space demanding reaction in the solid state.[17,18] On the basis of these arguments, it seems appropriate to analyze in detail the crystal packing and free cavity space of Fe(stpy)$_4$(NCSe)$_2$ to get more insight into the possibility for a solid-state photoisomerization. We have mentioned in the experimental section that it has not been observed from photocrystallographic techniques, most probably because appropriate excitation conditions could not have been realized. We should mention at this point that we have detected a photoinduced effect on the solid state using a 534 nm excitation, namely, a large unit cell increase at room temperature. We believe this is related to a different process, which will be reported thoroughly in a forthcoming paper.

First insights of the packing effects in the all-cis and all-trans isomers of the title compound are provided by an inspection of the unit cell volume per metal ion (or molecular volume V_{mol}) as a function of the temperature, spin state, and configuration of the stpy ligand. As a matter of fact, the molecular volume of the trans isomer is ca. 3.4% larger than the molecular volume for the cis form at 293 K (both being in the high spin state at that temperature), corresponding to a much less dense crystal packing. A similar trend, although to a lesser extent, has been observed for the sulfur counterparts (molecular volume difference of 1%). Upon a temperature decrease to 104 K, the all-trans compound undergoes the spin transition, accompanied by a unit cell volume contraction. Accordingly, the cis$-$trans molecular volume difference reduces to 0.95%. Assuming similar 293$-$104 K thermal contraction effects for the two forms, the molecular volume change attributed to the spin crossover itself can thus be estimated to be ca. 2%, which is within the accepted range for typical spin-crossover materials.[7,14] The comparison between the two sets of data shows that the unit cell reorganization associated with a formal substitution of the stpy isomer is almost equally sterically demanding than the spin-crossover itself, which may be of interest with regard to the trans$-$cis transformation of coordinated stpy.

As recently suggested by Moorthy and co-workers,[19] the spatial distribution and volume of free cavities in the crystal packing may be very informative if one wants to understand a specific solid-state reaction process. For instance, the voids in the crystal lattice of cis derivatives of styrylcoumarins are located in specific positions which permit the structural reorganizations to the trans forms.[19] The free cavities in the cis and trans isomers of Fe(stpy)$_4$(NCSe)$_2$ have been defined using PLATON[20] as the region of the unit cell which could accommodate probe spheres of a chosen radius ($0.7 \le r \le 1.2$ Å) not entering the van der Waals surfaces of neighboring atoms. It is found that the crystal lattice of Fe(stpy)$_4$(NCSe)$_2$ contains a large fraction of void space (~11% at r = 0.8 Å, for all-trans and all-cis species), compared for example with the photoactive *cis*-styrylcoumarins (~1$-$4% at r = 0.8 Å). On the contrary, the location of the voids does not necessarily fit with the putative position of the phenyl rings of each stpy ligand after cis → trans and trans → cis isomerizations.

We should stress that the crystal structures of all-cis and all-trans complexes we derived here correspond to the

(16) (a) Weiss, R. G.; Ramamurthy, V.; Hammond, G. S. *Acc. Chem. Res.* **1993**, *26*, 530. (b) Hashizume, D.; Ohasi, Y. *J. Chem. Soc., Perkin Trans. 2* **1999**, *8*, 1689. (c) Sawada, K.; Hashizume, D.; Sekine, A.; Uekusa, H.; Kato, K.; Ohasi, Y.; Kakinuma, K.; Ohgo, Y. *Acta Crystallogr.* **1996**, *B52*, 303.
(17) Kaupp, G.; Haak, M. *Angew. Chem., Int. Ed. Engl.* **1996**, *35*, 2774.
(18) Natarajan, A.; Mague, J. T.; Venkatesan, K.; Arai, T.; Ramamurthy, V. *J. Org. Chem.* **2006**, *71*, 1055.
(19) Moorthy, J. N.; Venkatakrishnan, P.; Savitha, G.; Weiss, R. G. *Photochem. Photobiol. Sci.* **2006**, *5*, 903.
(20) Spek, A. L. *PLATON*; Utrecht University: Utrecht, The Netherlands, 2005.

crystal phases obtained in solution by solvent evaporation. We do not expect that the cis → trans photoisomerization would result in the observed all-trans complex crystal structure, and similarly for the trans → cis transformation. This is particularly evident owing to the very different crystal packing of both isomers.

3. Dispersion of $Fe(stpy)_4(NCSe)_2$ within PMMA and Thin Film Processing. Transparent and semirigid PMMA thin films containing an increasing amount of iron(II) complexes (2−20 wt %) were prepared by spin-coating techniques from a mixture of PMMA and complex solutions. The spin-crossover molecule so incorporated in the polymer host can be considered as a probe of surrounding effects. A distribution of environments for $Fe(stpy)_4(NCSe)_2$ was pointed out from a careful analysis of our optical MCD measurements.[10] The literature concerning strongly luminescent molecular compounds[21,22] in the form of doped PMMA films provides strong evidence for the coexistence of dispersed (weakly interacting) and aggregated (strongly interacting) molecules. The formation of aggregates was related both to specific intermolecular interaction (for example π-stacking) and processing characteristics (concentration, cosolvent, thermal treatment, etc.). According to that, we have performed scanning electron microscopy measurements to probe the nature of heterogeneities within the doped PMMA thin films. A low accelerating voltage (ca. 1 kV) was selected, and the focus was continuously increased until a threshold corresponding to the polymer damage was reached. Under these conditions, the experiments show no molecular aggregates with sizes larger than ∼100 nm. It is thus assumed that the above-mentioned heterogeneities, the thin film transparency, and the rather similar spin-crossover curves centered at 163 K (microcrystalline solid) and 135 ± 25 K (doped thin film) are due to a fraction of complexes in the form of small aggregates within PMMA (average size ≤ 100 nm).

4. Optical and Photochemical Measurements on PMMA Films. The optical absorptions of the doped thin films (with 2−20 wt % of $Fe(stpy)_4(NCSe)_2$) were shown to be linearly correlated to the iron(II) complex concentrations. In the following, the photoisomerization and photomagnetic properties have been investigated with the 5% doped thin film, that is, one of the less absorbing materials.

As previously described,[10] the absorption spectra of 5% doped thin films show in the UV region the intense $\pi-\pi^*$ absorptions of the styrylpyridine characterizing each isomer in all-cis and all-trans complexes.[6] These bands are slightly red-shifted and broadened in comparison to those of the base-free ligands in PMMA. This is indicative of specific conformational and vibrational characteristics of coordinated stpy. It also arises from the convolution on the low-energy side with the metal-to-ligand charge transfer bands of relatively weak intensity (ca. 420 nm for all-cis complex). These MLCT absorptions are obviously related to the metal ion spin state

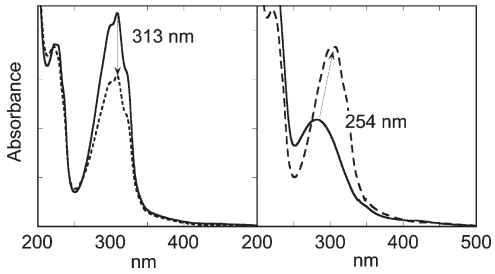

Figure 5. UV−vis spectra (at 120 K) of thin films doped with all-trans (left) and all-cis (right) complexes. Initial sample (−) and photostationary state (−−) observed after UV illumination with 313 nm (left) or 254 nm (right) wavelength.

and its conversion upon the spin-crossover process (see Figure S2 for all-trans complex, Supporting Information). Because of the weak variation observed here, we took advantage of the UV−vis MCD study performed on similar doped polymeric thin films.[10] The magnetic states of all-cis and all-trans complexes in highly diluted films were precisely determined in a large temperature range (2−200 K). In comparison to the microcrystalline environment, the all-trans compound in polymeric films exhibits a similar spin-crossover curve but localized in the low-temperature range ($T_{1/2}$ = 135 ± 25 K). We have selected a working temperature of 120 K for the photochemical investigation and 130 K for the photomagnetic investigation. At these temperatures, the iron(II) complexes within the doped thin films are either in the HS state (all-cis) or partly in the LS state (all-trans, spin crossover range ca. 50−170 K).

Figure 5 shows the spectra of complexes recorded before and after the thin films' irradiation (120 K, $\lambda_{cis\rightarrow trans}$ = 254 nm and $\lambda_{trans\rightarrow cis}$ = 313 nm). Analogous experiments performed at room temperature with the base-free ligand in doped PMMA films indicate significant cis-to-trans and trans-to-cis configurational changes within the complexes. The all-trans transformation proceeds more slowly than the all-cis one.

The embedding of all-trans and all-cis complexes within PMMA thin films allows the bidirectional trans−cis photoisomerization of the photoactive stpy ligands to be observed at 120 K. Despite the overlap of cis−trans absorptions, the 254 nm excitation produces a photostationary state associated with a significant cis → trans transformation.

5. Photomagnetic Measurements of 5% Doped PMMA Films. The magnetization versus temperature data were collected on the starting material first in darkness (Figure S3, Supporting Information). The measurements were pursued at 130 K in the presence of a 355 nm excitation delivered by a YAG laser. Irradiations were stopped after the formation of photostationary states, and in the last sequence, the magnetization versus T data were recorded on the so-transformed polymeric film (in Figure S3, Supporting Information). The kinetics of transformations at 130 K are shown in Figure 6. The observed tendencies are (i) an increase of the metal ion magnetization during the trans-to-cis isomerization of stpy isomers, (ii) a decrease of magnetization during the reverse photoreaction, and for both samples (iii) a related modification of the magnetic behavior observed in a

(21) (a) Mao, C.-H.; Hong, J.-L.; Yeh, A.-C. *J. Polym. Sci.* **2008**, *46*, 631. (b) Su, F.-K.; Hong, J.-L.; Lin, L.-L. *J. Appl. Polym. Sci.* **2008**, *107*, 134.
(22) Fakis, M.; Polyzos, I.; Tsigaridas, G.; Giannetas, V.; Persephonis, P. *Phys. Rev. B* **2002**, *65*, 195203.

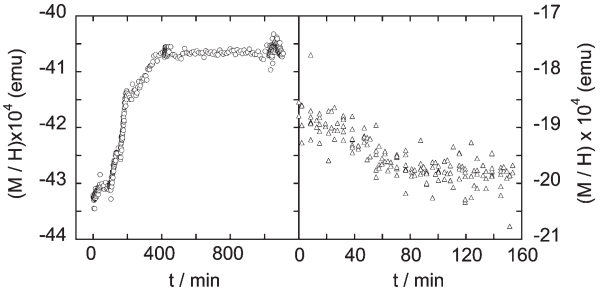

Figure 6. Magnetization/H vs the time of irradiation (355 nm, 130 K) for the thin films samples doped with all-trans (left, $H = 5000$ Oe) and all-cis (right, $H = 1000$ Oe) complexes.

range of temperature. These features support the following outcome:

$$\underset{\text{HS}}{\text{all} - \text{cis Fe(II)}} \leftrightarrow \underset{\text{LS}}{\text{all} - \text{trans Fe(II)}}$$

We note first that this follows the expectation based on the MCD and magnetic data collected with thin films and bulk samples, respectively. The trans−cis isomerization of the organic moieties induces a sufficient modulation of the metal ion's electronic environment to switch the magnetic behavior of both LD-LISC iron(II) isomers. The bidirectional photomagnetic behavior is detected here by direct magnetic measurements of doped PMMA thin films.

As established above, probing the reversibility of the sample transformation requires the use of two very distinct excitation wavelengths, in order to form two photostationary states enriched with each of the photoisomers. This experiment cannot be achieved with our setup for SQUID in situ irradiation.

Whereas magnetic and optical measurements provide nice evidence of LD-LISC activity within polymeric matrices, they are clearly not appropriate for probing the nature of the photostationnary states and the mechanism. MCD spectroscopy coupled to time-resolved measurements might be especially interesting in this regard.

Conclusions

It is first confirmed that the electronic and magnetic properties of $Fe(stpy)_4(NCSe)_2$ complexes—in the form of crystalline samples—markedly depend on the stilbenoid configurations, that is, a prerequisite for a LD-LISC activity. Below 130 K, the polycrystalline solids show a dia- or paramagnetic behavior of the metal ion according to the all-trans and all-cis configurations of stpy ligands, respectively. The crystal structures show that the coordination of four styrylpyridines to Fe^{II} in the meridional plane imposes a low symmetry of the $[FeN_6]$ core, tilted pyridine rings, and distinct stilbenoid configurations. This feature restricts the π-stacking interactions with stpy parallel configurations, and thus all-cis and all-trans lattices are stabilized by rather weak contacts involving NCSe and stpy groups. The cis−trans molecular volume difference and the free cavities in both all-trans and all-cis solids have been analyzed, and some inferences have been drawn with regard to the photoactivity of the crystalline solids.

UV photoexcitation attempts of single crystals and powder monitored by crystallographic techniques were unsuccessful, and consequently the Fe^{II} compounds were dispersed in polymer thin films for probing their LD-LISC activity. The cis−trans isomerizations of the stilbenoid moieties were observed at a temperature of 120 K, at which the Fe^{II} compounds dispersed in PMMA are either in the high-spin state (all-cis) or partly in the low-spin state (all-trans). When the photoexcitation was carried out within the SQUID magnetometer, a detectable gain (reduction) of the 130 K magnetization was resolved; this is related to the trans-to-cis (cis-to-trans) stpy isomerization. This finding obtained with the highly doped thin films nicely fits the expectations based on the very first MCD investigations of similar polymer films and also the all-trans and all-cis bulk properties.

The LD-LISC process reported here for $Fe(stpy)_4(NCSe)_2$ opens the way for investigating reversible photoswitching in crystalline solids. The crystalline LD-LISC activity of $Fe(stpy)_4(NCSe)_2$ is currently explored with visible light excitation and specific detection techniques.

A very promising approach consists of the combination of the spin-crossover moiety with a diarylethene-type ligand. In contrast to stilbenoid-type ligands, the diarylethene molecules present good photochromic properties and relatively small associated structural changes. Some of us have reported the very first result obtained along this line.[23] The elaboration of such LD-LISC systems is under way.

Acknowledgment. We thank François Brisset for acquiring SEM images, Joelle Sainton and Katell Sénéchal-David for their assistance. This work was supported by the CNRS, the French Ministry of Research, MAGMA-Net NoE of the European Union (contract: NMP3-CT-2005-515767-2).

Supporting Information Available: X-ray crystallographic files in CIF format for compounds $Fe(\textit{trans}\text{-}stpy)_4(NCSe)_2$ and $Fe(\textit{cis}\text{-}stpy)_4(NCSe)_2$, full tables of structural parameters, magnetic study of the $S = 2$ state for the all-cis powder, and magnetic and optical characterizations of doped PMMA thin films. This material is available free of charge via the Internet at http://pubs.acs.org.

(23) Sénéchal-David, K.; Zaman, N.; Walko, M.; Halza, E.; Rivière, E.; Guillot, R.; Feringa, B. L.; Boillot, M.-L. *Dalton Trans.* **2008**, 1932.